Nonresonant Inelastic X-Ray Scattering and Energy-Resolved Wannier Function Investigation of *d-d* Excitations in NiO and CoO

B. C. Larson,[1] Wei Ku,[2] J. Z. Tischler,[1] Chi-Cheng Lee,[2,3] O. D. Restrepo,[1,4] A. G. Eguiluz,[1,4]
P. Zschack,[5] and K. D. Finkelstein[6]

[1]*Materials Science & Technology Division, Oak Ridge National Laboratory, Oak Ridge, Tennessee 37831, USA*
[2]*Department of Physics, Brookhaven National Laboratory, Upton, New York, 11973, USA*
[3]*Department of Physics, Tamkang University, Tamsui, Taiwan 25137, Republic of China*
[4]*Department of Physics & Astronomy, University of Tennessee, Knoxville, Tennessee 37996, USA*
[5]*XOR/UNI, Advanced Photon Source, Argonne National Laboratory, Argonne, Illinois 60439, USA*
[6]*Cornell High Energy Synchrotron Source, Cornell University, Ithaca, New York 14853, USA*

Nonresonant inelastic x-ray scattering measurements on NiO and CoO show that strong dipole-forbidden *d-d* excitations appear within the Mott gap at large wave vectors. These dominant excitations are highly anisotropic, and have [001] nodal directions for NiO. Theoretical analyses based on a novel, energy-resolved Wannier function (within the local density approximation + Hubbard *U*) show that the anisotropy reflects the local exciton wave functions and local point-group symmetry. The sensitivity to weak symmetry breaking in particle-hole wave functions suggests a wide application to strongly correlated systems.

PACS numbers: 71.27.+a, 61.10.Eq, 71.15.−m, 71.35.−y

Strongly correlated transition-metal oxides (e.g., manganites, cobaltates, and cuprates) display a wide array of fundamentally and technologically important properties ranging from colossal magnetoresistance to high temperature superconductivity. Accordingly, transition-metal oxides are of strong experimental and theoretical interest, and simple transition-metal monoxides are of particular interest as prototype systems [1–5]. The principal scattering tools for investigating dipole-forbidden *d-d* excitations in transition-metal monoxides have been soft x-ray emission spectroscopy [1], soft resonant inelastic x-ray scattering (RIXS) [2], and spin-polarized electron energy loss spectroscopy [3]. Exploiting parity relaxation and the increased intensities associated with resonant inelastic scattering, detailed information has been obtained on *d-d* multiplets and charge-transfer [5] excitations with the aid of configuration-interaction cluster model analyses [1–5].

High-energy (*K* edge) RIXS [6] has become an important technique for investigations of strongly correlated electronic effects in (highly absorbing) rare earth cuprates [7,8] and manganites [9], where the large momentum transfers probe with real-space resolution commensurate with the spatial extent of the excitations [4]. However, relating RIXS measurements to the dynamical structure factor [9,10] remains a challenge [10–12] compared with the first-principles relationship that exists for nonresonant inelastic x-ray scattering (NIXS) measurements [13,14] of core and valence excitations.

In this Letter, we exploit the atomic-scale resolution afforded by hard x-ray inelastic x-ray scattering and the simplicity of *nonresonant* linear response processes [13–15] in combination with energy-resolved Wannier function analyses to demonstrate a new and powerful technique for

probing the physics of *d-d* excitations in transition-metal monoxides. We present absolute NIXS measurements for NiO and CoO showing that sharp, dipole-forbidden *d-d* excitations appear within the Mott gap at large **q** (wave vector) and, further, that their intensities dominate the loss spectra at large *q*. Even more remarkable is the fact that the intensity of these *d-d* excitations is highly anisotropic in **q**, with [001] nodal directions for NiO. We show by a novel theoretical analysis employing first-principles energy-resolved Wannier functions that NIXS measurements of local excitons probe the particle-hole wave functions *directly* and that the strong anisotropy is intimately tied to the cubic point-group symmetry of the wave functions. Moreover, the absence of a nodal direction for CoO shows NIXS measurements to be very sensitive to weak symmetry breaking.

The measurements in this study were performed on polished single crystals of NiO and CoO with ⟨001⟩ or ⟨111⟩ orientations for wave vectors ranging from $q \sim 2$ to 7 Å^{-1} both along and between the [001], [111], and [110] directions. Measurements were made with 7.59 keV incident x rays at 1.1 eV resolution [Figs. 1(a) and 1(b)] using the high heat-load 111 Si monochromator in combination with a spherically bent Ge 444 analyzer (~ 0.3 Å^{-1} q resolution) on the XOR/UNI ID-33 undulator beam line at the Advanced Photon Source (APS). Higher-resolution (0.3 eV) measurements were made initially on the C-1 beam line at the Cornell High-Energy Synchrotron Source (CHESS) and detailed high-resolution measurements [Figs. 2(a) and 2(b)] were made using channel-cut postmonochromators on the XOR/UNI ID-33 beam line at the APS. The non-negligible tails of the quasielastic peak near $\Delta E = 0$ were determined (and removed) by scaling
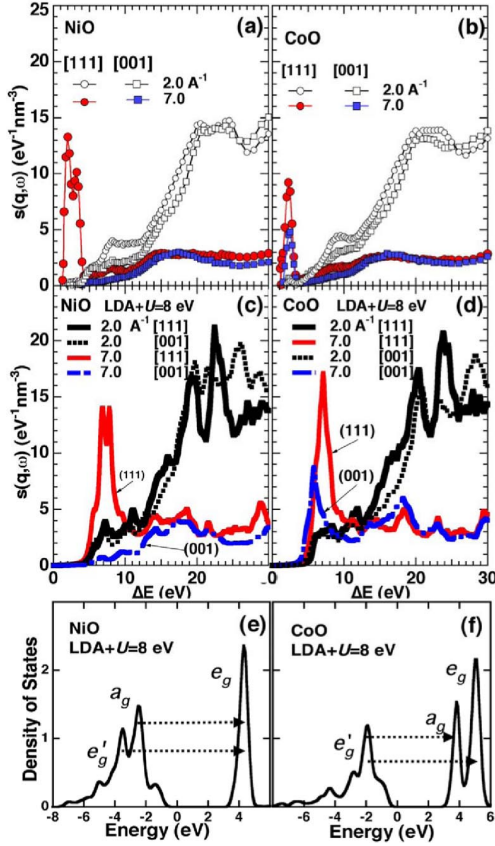
FIG. 1 (color online).   Low-resolution (1.1 eV) NIXS measurements and LDA $+ U$/RPA calculations of the dynamical structure factor for NiO and CoO: (a),(b) measurements along the 001 and 111 directions for NiO and CoO; (c),(d) calculations along the 001 and 111 directions for NiO and CoO; (e),(f) single-particle density of states for NiO and CoO within LDA $+ U$, where the dotted arrows indicate sharp d-d transitions between the upper and lower Hubbard bands in NiO and CoO.
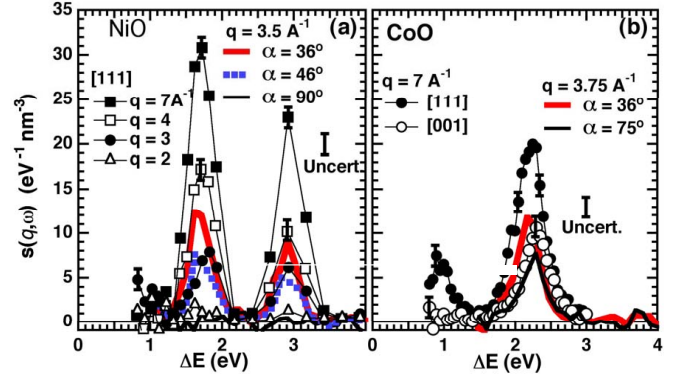

FIG. 2 (color online).   High-resolution (0.3 eV) measurements of the q magnitude and orientation dependence of the d-d peak excitations for NiO and CoO; α is the q-orientation angle between the 110 and 001 directions [see Figs. 4(f) and 4(h)].

formed in this study within the RPA approximation of LDA $+ U$ ($U = 8$ eV) using all-electron, linearized augmented plane wave (LAPW) electronic structure. Overall, the small-q gap widths and the strength of the calculated dynamical response are in good agreement with the measured intensities out to 30 eV, considering the lack of decay and lifetime effects within the theory.

For large wave vectors, where quadrupole and higher multipole scattering come into play, strong dipole-forbidden d-d excitations are found in the Mott gaps for both NiO and CoO. Both the low-resolution measurements in Figs. 1(a) and 1(b) for $q = 7$ Å^{-1} and the higher-resolution (~ 0.3 eV) measurements in Figs. 2(a) and 2(b) show that nondispersive (to within ~ 0.1 eV) d-d excitations appear at energies of 1.7 and 2.9 eV for $q > 2$ Å^{-1} in the [111] direction in NiO, and at 1 and 2.3 eV at large q for both the [001] and [111] directions in CoO. From the width of the measured peaks in Fig. 2, the intrinsic energy width of the d-d excitations is estimated to be ~ 0.3 eV. We note that the (0.3 eV resolution) d-d peak intensities in Fig. 2 are fully an order of magnitude stronger than the slowly varying continuum loss spectra above the gap for large q in Fig. 1. Remarkably, the LDA $+ U$/RPA loss spectra calculated for NiO and CoO at $q = 7$ Å^{-1} in Figs. 1(c) and 1(d) are dominated by similarly sharp and orientationally anisotropic peaks, but they appear at energies of ~ 6–8 eV rather than the 1–3 eV peak positions measured for NiO and CoO.

Using the single-particle density of states spectra in Figs. 1(e) and 1(f) and detailed spectral analysis of the response calculations, the NiO peaks have been identified as primarily Ni d-d ($a_g \rightarrow e_g$) and ($e'_g \rightarrow e_g$) excitations, and the CoO peaks are Co d-d ($e'_g \rightarrow a_g$) and ($e'_g \rightarrow e_g$) excitations. Since particle-hole attraction is absent in these RPA response calculations, the ~ 5 eV difference between the measured and calculated energies provides a rough estimate of the particle-hole binding energies. The presence of only two (clean) nonresonant d-d excitations is in striking contrast to the complex multiplet structures typi-

quasielastic peak measurements on CaF$_2$ to the quasielastic peak heights of measurements on NiO and CoO. The ~ 13 eV optical gap of CaF$_2$ provides a window to measure the (resolution broadened) quasielastic scattering tail of the spectrometer system directly, out to ~ 10 eV. The measurements (Figs. 1 and 2) were reduced to absolute units of eV^{-1}nm^3 by scaling an f sum-rule calibration of the scattering system for aluminum by μ_{TMO}/μ_{Al}, where μ_{TMO} is the linear absorption coefficient of NiO or CoO and μ_{Al} is the linear absorption coefficient for Al, as described previously [15].

Figures 1(a) and 1(b) show the results of *absolute* NIXS measurements of $s(\mathbf{q}, \omega)$ at $q = 2$ Å^{-1} and 7 Å^{-1} along [001] and [111] directions of NiO and CoO. The results for $q = 2$ Å^{-1} (open symbols) show the well-known [4,5] ~ 4 eV charge-transfer gaps for both NiO and CoO, with continuum particle-hole spectral structure in the ~ 7–10 eV range and broad loss peaks in the ~ 20–25 eV range as discussed elsewhere [16,17]; dipole-forbidden d-d excitations are not visible in this small-q range. Figures 1(c) and 1(d) show $s(\mathbf{q}, \omega)$ calculations [17] per-

cally observed in resonant scattering measurements [1–4,18]; this reflects the fundamental difference in the microscopic processes involved, as only linear charge response is involved in NIXS.

Of particular interest in this Letter, though, is the fact that the *d*-*d* intensities measured by NIXS depend strongly on the orientation of the momentum transfer **q**. As shown above [Figs. 1(a), 1(b), 2(a), and 2(b)], the on-site *d*-*d* excitations for both CoO and NiO lose spectral weight dramatically on going from the [111] to the [001] directions; indeed, we find the [001] direction to be a nodal intensity direction for NiO.

We now demonstrate that this strong **q**-orientation anisotropy has important implications as a probe of strongly correlated electrons. The anisotropy contains fundamental information on local excitonic wave functions, a result that can be understood intuitively via a novel Wannier function real-space description discussed below. In the Wannier basis, the fully interacting susceptibility can be expressed formally in terms of the particle-hole (*p*-*h*) correlation function *L* as [19,20],

$$\chi(\mathbf{x}_1 t_1; \mathbf{x}_2 t_2) = \sum_{mnm'n'} M_{m',m}^{\mathbf{x}_1} L_{mn;m'n'}(t_1 t_2; t_1 t_2) M_{n',n}^{\mathbf{x}_2}, \quad (1)$$

where the sums range over all processes associated with the creation of local *p*-*h* pairs ($|n'\rangle$, $|n\rangle$) at position $\mathbf{x}_2$ and time t_2, with probability amplitude $M_{n',n}^{\mathbf{x}_2} \equiv \phi_{n'}^*(\mathbf{x}_2)\phi_n(\mathbf{x}_2)$, followed by the propagation of the *p*-*h* pairs, described by *L*, and finally the annihilation of local *p*-*h* pairs ($|m\rangle$, $|m'\rangle$) at $\mathbf{x}_1$ at a later time t_1 with probability amplitude $M_{m',m}^{\mathbf{x}_1}$. After Fourier transforming to ($\mathbf{q}, \omega$) space, one finds that for a strongly bound local exciton (e.g., deep in the gap) that is well isolated from (and thus weakly coupled to) other excitations, the dynamical structure factor *at the exciton frequency* ω_{exc} is dominated by contributions from the local *p*-*h* pair ($|p\rangle$, $|h\rangle$) that forms the exciton:

$$-s(\mathbf{q}, \omega = \omega_{\text{exc}})/2\hbar = \text{Im}\chi(\mathbf{q}, \omega_{\text{exc}})$$
$$\cong |M_{p,h}^{\mathbf{q}}|^2 L_{ph;hp}(\omega_{\text{exc}}) \quad (2)$$

Thus, the *angular dependence* of NIXS measurements provides a *direct probe* of the Fourier transform of the local particle-hole wave function, $M_{p,h}^{\mathbf{q}} \equiv \int e^{-i\mathbf{q}\cdot\mathbf{x}} M_{p,h}^{\mathbf{x}} d\mathbf{x}$.

To analyze the anisotropies, we constructed energy-resolved, symmetry-respecting, atomic-scale Wannier functions [21] for NiO and CoO [20] from all-electron LDA + U orbitals, using energy ranges restricted to the narrow widths of the sharp e_g', a_g, and e_g states in Figs. 1(e) and 1(f). Examples of the resulting Wannier functions are shown in Fig. 3 for the e_g (i.e., $|p\rangle$) and e_g' (i.e., $|h\rangle$) states in the spin-minority channel; the full shell of *d* states in the spin majority channel does not contribute to *d*-*d* charge excitations. The narrow energy widths ensure the Wannier functions to be either pure particle or pure hole states (i.e.,
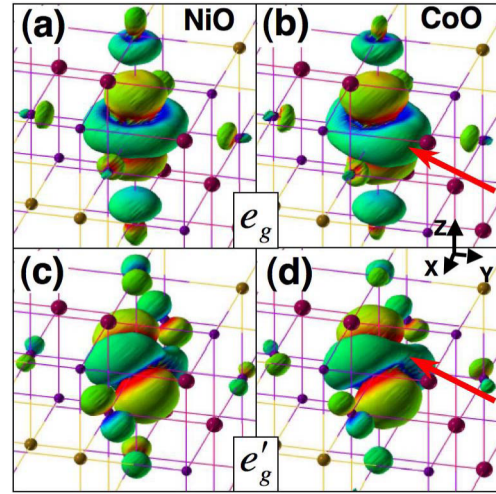

FIG. 3 (color online).   Cation *d*-state Wannier functions for e_g' and e_g states of NiO and CoO, showing oxygen-*p* hybridization. Note the bulge distortion (at arrow) in the CoO e_g state and the slightly less nodal shape for CoO in the e_g' state compared with the nearly cubic symmetry shapes for NiO.

either fully above or fully below the Fermi energy), and naturally incorporate the hybridization of Ni-*d* and O-*p* states within the energy, as observed in the distorted tails of the Wannier functions in Fig. 3.

The calculated oscillator strengths ($\propto |M_{h,p}^{\mathbf{q}}|^2$) corresponding to the ($e_g' \to e_g$) *p*-*h* pairs in Fig. 3 [averaged over cubic equivalent antiferromagnetic (AF) domains] are presented in Figs. 4(a)–4(d) in the form of 3D isovalue contours and 2D false-color slices of the 3D intensity distributions. We note first the dipole-forbidden nature of the excitations indicated by the hollow (zero intensity) centers of the intensity distributions (i.e., for $q < 2$ Å^{-1}) and the strong maxima around 7 Å^{-1} in [111] directions, as observed experimentally in Figs. 1 and 2. We emphasize, in particular, the strong anisotropies in the calculated intensity distributions: the nodes along the [001] directions for NiO, the analogous deep (but non-nodal) minima along [001] directions for CoO, and the relative minima along [110] directions for both materials. The maxima near $q \sim$ 7 Å^{-1} [outer dotted lines in Figs. 4(b) and 4(d)] along the [111] direction in the calculated oscillator strengths for both NiO and CoO reflect the *atomic scale* of the local excitons ($2\pi/q \approx 0.9$ Å). This result is in good agreement with the $q = 2, 3, 4,$ and 7 Å^{-1} NIXS measurements along the [111] direction in Fig. 2(a), plus low-resolution NIXS measurements (not shown) made using 9.49 keV x rays that indicate lower intensities at 8 and 9 Å^{-1}.

A direct comparison with the measured anisotropies for the ($e_g' \to e_g$) excitations in NiO ($\sim$2.9 eV; $q = 3.5$ Å^{-1}) and CoO ($\sim$2.3 eV; $q = 3.75$ Å^{-1}) can be seen in the polar plots in Figs. 4(e)–4(h). We note good agreement in the overall shapes of the measured and calculated anisotropies, in particular, the [001] nodal direction in NiO and the lack of an intensity node for CoO. Detailed analy-
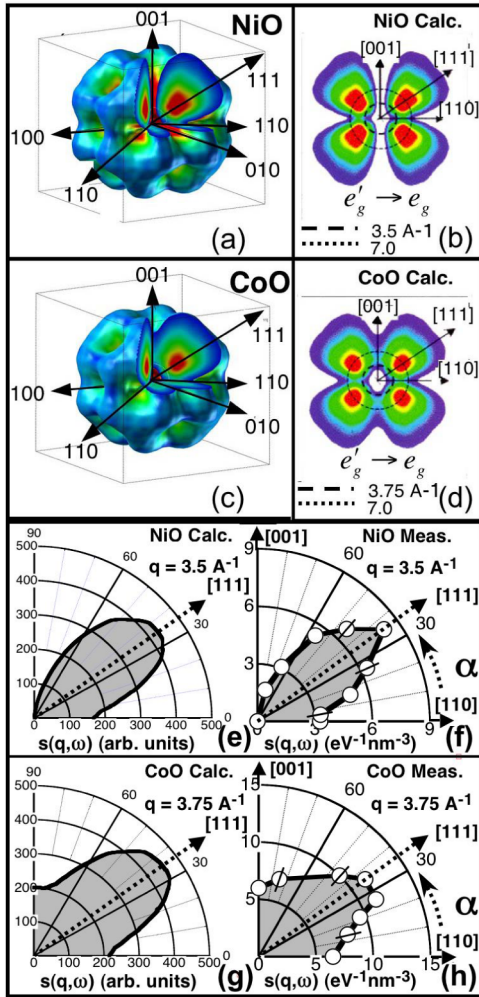
FIG. 4 (color online). Energy-resolved Wannier function analyses and NIXS measurements of the **q** dependence of *d-d* excitations in NiO and CoO: (a),(c) 3D color coded (red-high) plots of Fourier transformed ($e'_g \rightarrow e_g$) oscillator strengths for NiO and CoO; (b),(d) 2D color coded slices of (a),(c) in the (001 110) plane, where the inner dashed circles correspond to 3.5 and 3.75 Å^{-1} for NiO and CoO, respectively, and the outer dashed circle corresponds to 7 Å^{-1}; (e),(g) polar plots of the calculated *d-d* spectral weights for NiO and CoO on the inner circles of (b),(d); (f),(h) polar plots of the measured peak heights of the ($e'_g \rightarrow e_g$) excitations for NiO and CoO.

ses [19] of individual Wannier states has confirmed that the [001] nodal directions for NiO are a direct result of a "**q**-selection rule" associated with the nearly cubic point-group symmetry of NiO, which is known [22] to have a much smaller rhombohedral AF distortion than CoO. Accordingly, the lack of an intensity node for CoO reflects a breaking of cubic symmetry in the charge channel of CoO, thereby demonstrating NIXS to be a highly sensitive probe of symmetry breaking in the underlying states forming the excitations. The Wannier functions in Fig. 3 provide a real-space picture of the orbital distortions under broken symmetry; we note a bulge in the belt of the CoO e_g state and a slightly less nodal direction in the e'_g state of

CoO (see arrows). Similar analyses on the low-energy peaks are in progress.

In summary, we have observed strong local exciton peaks inside the Mott gap of NiO and CoO via large-*q* NIXS measurements. The highly anisotropic spectral weights of these atomic-scale excitons were shown to provide detailed information on the particle-hole wave functions when combined with energy-resolved Wannier function analyses, a direct connection that has not been exploited previously. The direct and absolute relationship between NIXS measurements and first-principles linear response theory plays a critical role in this capability, a tool that will find general application in fundamental investigations of strongly correlated systems like manganites, cuprates, and cobaltates.

[1] S. M. Butorin, J. Electron Spectrosc. Relat. Phenom. **110–111**, 213 (2000).
[2] L.-C. Duda *et al.*, Phys. Rev. Lett. **96**, 067402 (2006).
[3] B. Fromme, *d-d Excitations in Transition-Metal Oxides*, Springer Tracts in Modern Physics (Springer-Verlag, New York, 2001), Vol. 170.
[4] A. Kotani, Eur. Phys. J. B **47**, 3 (2005).
[5] J. Zaanen and G. A. Sawatzky, J. Solid State Chem. **88**, 8 (1990).
[6] C.-C. Kao *et al.*, Phys. Rev. B **54**, 16 361 (1996).
[7] J. P. Hill *et al.*, Phys. Rev. Lett. **80**, 4967 (1998).
[8] P. Abbamonte *et al.*, Phys. Rev. Lett. **83**, 860 (1999).
[9] S. Grenier *et al.*, Phys. Rev. Lett. **94**, 047203 (2005).
[10] J. van den Brink and M. van Veenendaal, J. Phys. Chem. Solids **66**, 2145 (2005).
[11] P. M. Platzman and E. D. Isaacs, Phys. Rev. B **57**, 11 107 (1998).
[12] K. Tsutsui, T. Tohyama, and S. Maekawa, Phys. Rev. Lett. **91**, 117001 (2003).
[13] K. Hämäläinen and S. Manninen, J. Phys. Condens. Matter **13**, 7539 (2001).
[14] T. T. Fister *et al.*, Rev. Sci. Instrum. **77**, 063901 (2006).
[15] J. Z. Tischler *et al.*, Phys. Status Solidi A **237**, 280 (2003).
[16] F. Aryasetiawan *et al.*, Phys. Rev. B **50**, 7311 (1994).
[17] A. G. Eguiluz *et al.*, J. Phys. Chem. Solids **66**, 2281 (2005).
[18] G. Ghiringhelli *et al.*, J. Phys. Condens. Matter **17**, 5397 (2005).
[19] G. Baym and L. P. Kadanoff, Phys. Rev. **124**, 287 (1961).
[20] C.-C. Lee, H.-C. Hsueh, and Wei Ku (to be published).
[21] W. Ku *et al.*, Phys. Rev. Lett. **89**, 167204 (2002).
[22] W. Jauch and M. Reehuis, Phys. Rev. B **70**, 195121 (2004).